Fiducial Markers for Combined 3-Dimensional Mass Spectrometric and Optical Tissue Imaging

Kamila Chughtai,[†] Lu Jiang,[‡] Tiffany R. Greenwood,[‡] Ivo Klinkert,[†] Erika R. Amstalden van Hove,[†] Ron M. A. Heeren,*[,†,§] and Kristine Glunde*[,‡,∥]

[†]FOM Institute AMOLF, Science Park 104, 1098 XG Amsterdam, The Netherlands

[‡]JHU ICMIC Program, The Russell H. Morgan Department of Radiology and Radiological Science, The Johns Hopkins University School of Medicine, 212 Traylor Building, 720 Rutland Avenue, Baltimore, Maryland 21205, United States

[§]The Netherlands Proteomics Centre, P.O. Box 80082, 3508 TB Utrecht, The Netherlands

[∥]Sidney Kimmel Comprehensive Cancer Center, Johns Hopkins University School of Medicine, Baltimore, Maryland 21231, United States

Supporting Information

ABSTRACT: Mass spectrometric imaging (MSI) has become widely used in the analysis of a variety of biological surfaces. Biological samples are spatially, morphologically, and metabolically complex. Multimodal molecular imaging is an emerging approach that is capable of dealing with this complexity. In a multimodal approach, different imaging modalities can provide precise information about the local molecular composition of the surfaces. Images obtained by MSI can be coregistered with images obtained by other molecular imaging techniques such as microscopic images of fluorescent protein expression or histologically stained sections. In order to properly coregister images from different modalities, each tissue section must contain points of reference, which are visible in all data sets. Here, we report a newly developed coregistration technique using fiducial markers such as cresyl violet, Ponceau S, and bromophenol blue that possess a combination of optical and molecular properties that result in a clear mass spectrometric signature. We describe these fiducial markers and demonstrate an application that allows accurate coregistration and 3-dimensional reconstruction of serial histological and fluorescent microscopic images with MSI images of thin tissue sections from a breast tumor model.

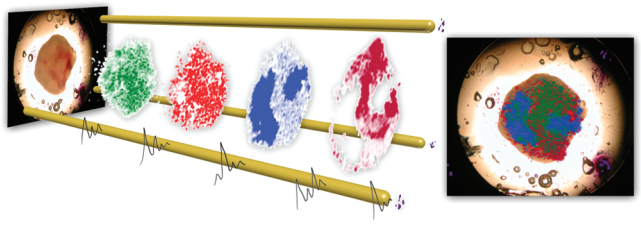

Multimodal biomedical imaging that incorporates mass spectrometric imaging (MSI) as one modality is a rapidly evolving discipline.[1,2] MSI offers a detailed insight into the molecular composition of complex biological surfaces such as single cells,[3] small histological sections,[4] and up to large whole rodent sections.[5] MSI does not require any *a priori* knowledge about the analyzed sample, which makes it a unique label free discovery technique.[6] MSI is an *ex vivo* technique, optimally suited for the analysis of thin tissue sections obtained with a standard cryo-microtome available in most pathology departments. Data acquisition is typically performed directly from 10 μm thick tissue sections using a mass spectrometer that is capable of acquiring a complete spectrum of molecular ions from each point within a predefined raster of *x*- and *y*-coordinates on the sample surface. Dedicated MSI software is used to generate molecular ion images from the acquired spectra that display the intensity distribution of any selected mass-to-charge ratio (m/z) of detected biomolecules over the imaged area. The integration of this molecular imaging approach into a clinical workflow requires the ability to compare and contrast the mass resolved images with conventional histological images. This integration of results obtained by methodologies from different disciplines assists in validating and interpreting normal and pathological molecular patterns as it brings together different pieces of information. Among the conventional histological imaging techniques are hematoxylin and eosin (H&E) staining, which visualizes morphological features of the tissue section, while an immunohistochemical (IHC) staining provides the detailed distribution of a selected protein known to be involved in a pathological cellular process. In biomedical research applications, the use of different fluorescent proteins[7] enables the investigation of protein expression, gene reporter activity, signaling pathways, oncogene activity, or cell tracking at low spatial resolution *in vivo*[8] or at higher spatial resolution in fresh tissue slices *ex vivo*.[9] Mass spectrometric images provide visualization of the distribution of a plethora of molecules that are spatially correlated with a region of interest or with a fluorescent or IHC-stained protein of interest.[1] The validation of this data requires an accurate overlay of the different imaging modalities. The accurate

coregistration of MSI and optical (fluorescent, H&E, and IHC) images needs proper alignment and scaling of all modalities. Fiducial markers can assist during processing of two-dimensional (2D) data sets obtained from multimodal imaging.

Fiducial markers are also needed for three-dimensional (3D) molecular mass spectrometric imaging, which requires accurate alignment of individual molecular images. In this approach, 3D molecular volumes of samples are generated by successive 2D MSI experiments of tissue sections that are cut with well-defined spacing throughout a biological sample (e.g., a tumor or an organ).[10,11] Correct alignment of individual MSI data sets is crucial for the reconstruction of 3D molecular volumes. If clear spatial molecular features are observed in the consecutive mass spectrometry (MS) generated molecular images, they can be used for spatial alignment. In some cases, researchers have used blockface optical images taken from the cryo-microtome mounted sample during sectioning, or obtained from target-mounted samples, to enable alignment.[12] In the case of 3D reconstruction of MSI detected distributions in a rodent brain, researchers benefited from the availability of an existing anatomical atlas, in which the anatomical structures found in the rodent brain are described in great detail.[12−14] However, in many other cases, samples lack known or visible spatial detail, which makes correct alignment and ion intensity normalization for 3D reconstruction as well as coregistration with histological images impossible without markers.

When combining bright field/fluorescence microscopy, histological staining, and MSI, the selection of suitable fiducial marker(s) is not trivial. Tissue fixation and sectioning can deform and shrink the tissue introducing differences in slice thickness and sectioning angle, which can compromise image coregistration, if markers are not used. Good markers must fulfill a number of requirements, such as intense color for microscopic bright field imaging applications, absorption/emission at selected wavelengths for fluorescence imaging, and good ionization for MSI. The fiducial markers should not diffuse during washing and matrix application procedures prior to MSI or histological staining and allow the coregistration of images acquired by different techniques. In addition, the fiducial markers should have good MALDI-MS properties. MALDI imaging is capable of visualizing molecules with good ionization properties even if they are present in the sample at a relatively low concentration.

Other groups have experimented with fiducial markers for multimodal imaging, but these are incompatible with mass spectrometry. Among them are metallic needles[15,16] or air-filled Teflon rods for imaging of tumor xenografts in rodents,[17] which can be positioned inside the tissue of interest prior to imaging. Visualized by magnetic resonance imaging (MRI) and positron emission tomography (PET) as well as histology and autoradiography on tissue sections, these rigid markers do not shrink with the surrounding tissue during fixation and displace and distort the tissue by their insertion. Ink based markers are more flexible and minimally disturb tissue structure during organ resection and sectioning.[18] The Bronze iridescent acrylic paint was found to be an appropriate fiducial marker for MRI at 7 T and for correlation of whole-specimen histopathology with MRI.[19,20] These methods require injection of the marker into living animals, which may affect tissue physiology as well as damage the tissue of interest, making them disadvantageous for common histological studies as well as making coregistration cumbersome.

We have developed and evaluated a new method that allows easy coregistration of different imaging modalities and 3D reconstruction using fiducial markers added adjacent to the tissue. We tested and optimized several fiducial markers such as cresyl violet, Ponceu S, and bromophenol blue, which do not interfere with sample preparation, exhibit good optical and fluorescent properties, are compatible with MS analysis, and serve as docking points for proper 2D/3D image alignment and for normalization of the individual 2D MS image intensities. This novel method is illustrated with an example of 3D multimodal imaging of human breast tumor xenograft models.

MATERIALS AND METHODS

Chemicals and Materials. The matrix α-cyano-4-hydroxycinnamic acid (CHCA) was purchased from Fluka (Switzerland), and ethanol, acetic acid, water, acetonitrile (ACN), and trifluoroacetic acid (TFA) were purchased from Biosolve (The Netherlands). Modified proteomics grade trypsin was purchased from Sigma (Germany). Cresyl violet acetate and Ponceau S were purchased from Sigma (U.S). Bromophenol blue was purchased from Bio-Rad (U.S.). Gelatin Type A was purchased from Sigma (U.S.). Mayer's hematoxylin was purchased from Sigma (U.S.) and aqueous Eosin Y from EMD Chemicals Inc. (U.S.). The Cytoseal 60 Mounting Medium, Richard-Allan Scientific was purchased from Thermo Scientific (U.S.).

Fiducial Marker Analysis: MALDI-MS. Cresyl violet acetate, Ponceau S, and bromophenol blue were prepared at a concentration of 10 mg/mL and dissolved in 100% ethanol (cresyl violet and bromophenol blue) or 1% acetic acid (Ponceau S). Marker solutions were mixed 1:1 with CHCA matrix prepared at a concentration of 10 mg/mL in 1:1 ACN:H_2O/0.1% TFA, and 1 μL of this solution was spotted on a MALDI target for MS analysis by MALDI-Q-TOF (Synapt HDMS, Waters, U.K.).

MALDI-MSI. Gelatin blocks were prepared using 15 × 15 × 5 mm^3 cryomolds (Sakura Finetek, U.S.). Cresyl violet acetate, Ponceau S, and bromophenol blue were prepared in 10% warm (37 °C) gelatin at a concentration of 10 mg/mL, and a 0.01 mL volume was injected into 10% gelatin blocks using a 1 mL syringe. Gelatin blocks were frozen at −20 °C for 30 min and sectioned into 20 μm thick sections using a cryo-microtome (HM525, MICROM, Germany). Two sections were mounted onto one 25 mm × 50 mm × 1.1 mm, Rs = 4−8 Ω indium tin oxide (ITO) coated slide (Delta Technologies, U.S.). CHCA matrix at a concentration of 10 mg/mL in 1:1 ACN:H_2O/0.1% TFA was applied on slides using an ImagePrep (Bruker, Germany). Samples were analyzed on a MALDI-Q-TOF (Synapt HDMS, Waters, U.K.) instrument in time-of-flight (TOF) mode detecting first positive and subsequently negative ions. The images were acquired at a spatial resolution of 150 μm × 150 μm. Data were visualized using BioMap software (Novartis, Basel, Switzerland).

Breast Tumor Imaging. The MDA-MB-231 breast cancer cell line was purchased from the American Type Culture Collection (ATCC) and genetically modified to express a red fluorescent protein (tdTomato) under the control of hypoxia response elements as previously described.[21,22] Cells were injected into the upper thoracic mammary fat pad of athymic nude mice (2 × 10^6 cells/injection), and tumor growth was monitored with standard calipers. When tumors reached a volume of approximately 500 mm^3, mice were sacrificed and tumors were removed. Each tumor was embedded into a gelatin

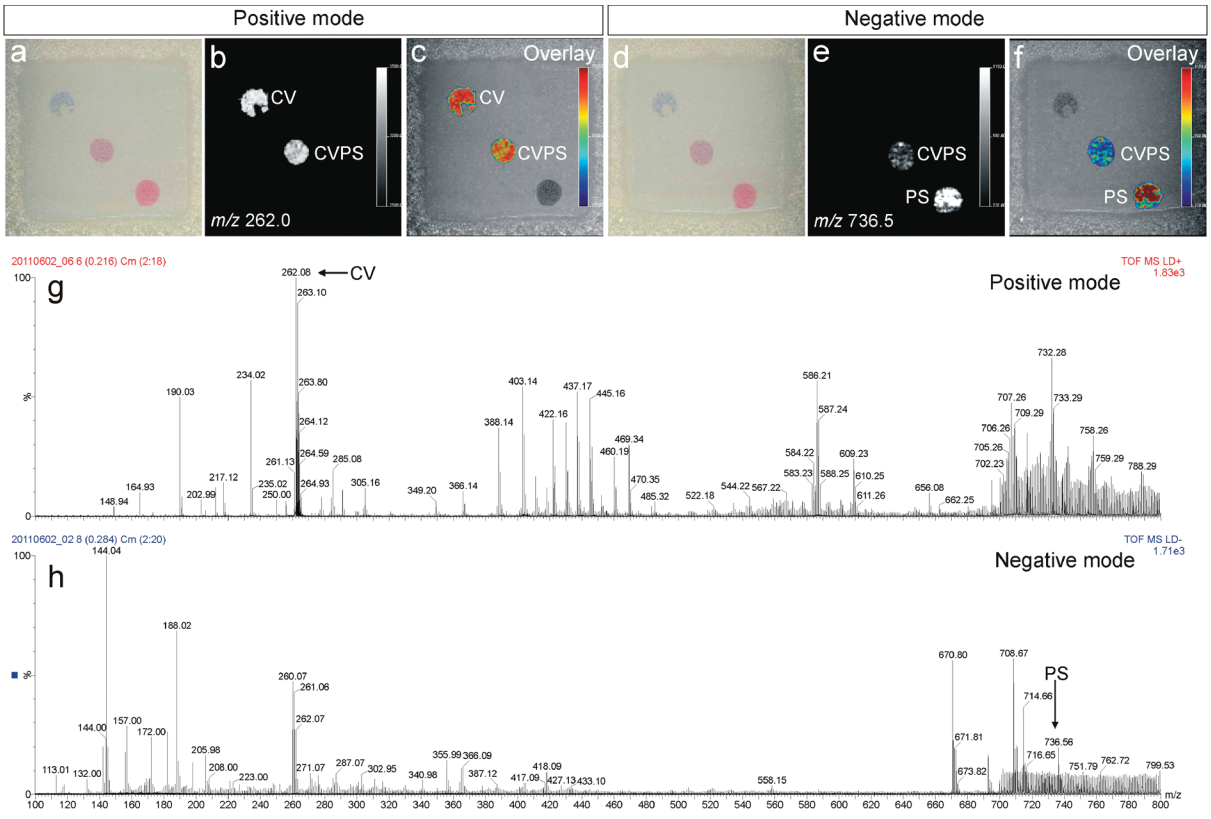

Figure 1. Optical images (a) and (d) show two adjacent sections taken from a gelatin block containing the injected fiducial markers: cresyl violet (CV), cresyl violet/Ponceau S (1:1) (CVPS), and Ponceau S (PS). Ion images were obtained in positive and negative ion mode. (b,c) Cresyl violet was detected at m/z 262.0 in positive ion mode. (e,f) Ponceau S was detected at m/z 736.5 in negative ion mode. The mixture of both markers (CVPS) was detected in both modes. (g) Spectrum showing the CV peak at m/z 262.0 detected from the CVPS mixture in positive ion mode. (h) Spectrum showing the PS peak at m/z 736.5 detected from the CVPS mixture in negative ion mode.

block (10% gelatin, cooled to 30 °C in order to prevent tissue degradation) and three cresyl violet fiducial markers were injected inside the block next to the tumor. The block was sectioned into serial 2 mm thick fresh tumor sections using an acrylic adjustable tissue slicer (12 mm depth up to 25 mm width; Braintree Scientific, Inc., Braintree, MA) and tissue slicer blades (Braintree Scientific, Inc.). These serial fresh tumor xenograft sections were each placed on individual microscope slides (Fisherbrand catalog number 12-550-34; Fisher Scientific, Pittsburgh, PA) and stored in an ice-box containing ice on the bottom, with the slides located on a perforated plate at approximately 1 cm above the ice to minimize tissue degradation. These fresh sections were imaged by bright field and fluorescence microscopy with a 1× objective attached to a Nikon inverted microscope, equipped with a filter set for 528–553 nm excitation and 600–660 nm emission and a Nikon Coolpix digital camera (Nikon Instruments, Inc., Melville, NY). Bright field imaging captured the position of the fiducial markers present inside the gelatin block as well as the shape of the tumor tissue. The fluorescence from tdTomato expression in hypoxic regions of these tumor sections was detected by fluorescence microscopy. The GNU Image Manipulation Program (GIMP 2.6) was used for 2D coregistration and overlay of bright field and fluorescence images of 2 mm thick tumor sections.

All 2 mm thick sections were snap-frozen immediately after microscopic imaging. From each 2 mm thick section, 10 μm thick sections were cut at −16 °C for MSI using a Microm HM550 cryo-microtome (Microm International GmbH, Walldorf, Germany) along with adjacent 10 μm thick sections for histological staining. Tissue sections for MSI analysis were mounted onto 25 mm × 50 mm × 1.1 mm, Rs = 4–8 Ω indium tin oxide (ITO) coated slides (Delta Technologies, U.S.) and for histological staining onto Superfrost Slides (VWR International, catalog no. 48311-600).

Before MSI analysis, tissue sections were briefly washed by immersion in 70% and 90% ethanol and dried in a vacuum desiccator for 10 min. Trypsin was resuspended in water at a concentration of 0.05 μg/μL, and a 5 nL per spot in a 150 μm × 150 μm raster was deposited by CHIP (Shimadzu, Japan). CHCA matrix was prepared at a concentration of 10 mg/mL in 1:1 ACN:H_2O/0.1% TFA and was applied by an ImagePrep (Bruker, Germany) application system. Samples were analyzed on a MALDI-Q-TOF (Synapt HDMS, Waters, U.K.) instrument in time-of-flight (TOF) mode detecting the positive ions. The images were acquired with 150 μm × 150 μm spatial resolution. For 2D MSI analysis and overlay of images, data were visualized using BioMap software (Novartis, Basel, Switzerland). 3D multimodal imaging reconstruction and registration was performed using a previously developed software platform,[23] which was written in Matlab (Natick, MS), and using Amira software for 3D visualization and volume rendering (Visage Imaging, Inc.).

H&E Staining Method. Tissue sections were stained using a modified H&E staining protocol as previously described. Briefly, 10 μm sections attached to Superfrost Slides (VWR International, catalog no. 48311-600) were washed with phosphate buffered saline (PBS), fixed with 3% paraformalde-

hyde for 30 min, washed with distilled water (dH_2O), and treated with Mayer's hematoxylin for 30 min at room temperature, followed by 5 washes with dH_2O. Sections were immediately immersed in aqueous Eosin Y for 30 min, followed by five washes with dH_2O, mounting with aqueous mounting medium, and attaching of a coverslip. Bright field images of H&E stained sections were acquired using a 1× objective attached to a Nikon microscope, equipped with a Nikon Coolpix digital camera (Nikon Instruments, Inc., Melville, NY).

RESULTS AND DISCUSSION

Mass Spectrometric Analysis of Fiducial Markers. We investigated MALDI-TOF-compatible fiducial marker compounds compatible with our optical microscopy protocols. Three different compounds were selected as good fiducial markers since they ionized easily during MALDI-MS and exhibited good optical properties. The spectra of these three compounds were obtained in positive ion mode (Figure S-1 in the Supporting Information). Encircled peaks correspond to cresyl violet (CV) $[M - CH_3COO^-]^+$ at m/z 262.0 in positive ion mode (Figure S-1a in the Supporting Information), Ponceau S (PS) did not ionize in positive ion mode (Figure S-1b in the Supporting Information), and bromophenol blue (BB) $[M + H]^+$ was detected at m/z 670.7 in positive ion mode (Figure S-1c in the Supporting Information).

The spectra of the fiducial markers were also obtained in negative ion mode (Figure S-2 in the Supporting Information). CV (Figure S-2a in the Supporting Information) did not ionize in negative ion mode, and PS $[M - Na]^-$ gave a signal at m/z 736.5 in negative ion mode (Figure S-2b in the Supporting Information). BB $[M - H]^-$ was detected at m/z 668.4 in negative ion mode (Figure S-2c in the Supporting Information).

Mass Spectrometric Imaging of Fiducial Markers. Three different fiducial markers were selected based on their intense colors for easy detection by microscopic imaging and compatibility with MSI. After resuspending the markers in gelatin and injection into a gelatin block, CV displayed violet color, PS dark red, and BB dark blue (Figure S-3a in the Supporting Information). After freezing and during cryosectioning of the block, the colors of these markers remained unchanged. During matrix application, due to the acidic pH of the matrix solution, BB changed its color to yellow (Figure S-3b in the Supporting Information).

Two adjacent sections from the gelatin block were subjected to MSI analysis, one in positive and one in negative ion mode. The ion images of different dye markers were coregistered with the corresponding optical images of the gelatin block sections (Figure S-3c–h in the Supporting Information). Following analysis in positive mode, ion images were obtained from the fiducial markers of CV at m/z 262.0 and BB at m/z 670.7 (Figure S-3c,e in the Supporting Information). No signal was detected from the PS marker (Figure S-3d in the Supporting Information).

The adjacent section of the gelatin block was analyzed in negative ion mode. No signal was detected from the CV marker (Figure S-3f in the Supporting Information), while signals from PS at m/z 736.5 and BB at m/z 668.4 were detected (Figure S-3 g,h in the Supporting Information). The results are summarized in Table S-1 in the Supporting Information.

Two fiducial markers, CV and PS, were selected for further analysis because they displayed good visibility in optical imaging and complementary MSI properties. A gelatin block was injected with pure CV, a 1:1 mixture of CV and PS (CVPS), and pure PS. MSI analyses were performed on two adjacent block sections, one in positive and one in negative ion mode (Figure 1a–f). Ion images were obtained from CV in positive mode (Figure 1a–c) and PS in negative mode (Figure 1d–f) and from the mixture of both in both ion modes. The mixture shows clearly visible marker localization in both positive and negative ion modes.

In order to evaluate potential ion suppression effects, solutions of CV and PS were mixed in a 1:1 ratio, spotted on MALDI target with CHCA, and analyzed in positive and in negative ion mode, respectively (Figure 1g,h). The expected peaks of CV at m/z 262.0 in positive ion mode and of PS at m/z 736.5 in negative ion mode were detected. From this analysis we concluded that a 1:1 mixture of PS and CV directly resuspended in gelatin is the optimal fiducial marker for MS image coregistration, 3D reconstruction, and normalization if analysis requires detection of both positively and negatively charged ions.

Multimodal MSI of a Breast Tumor Xenograft Model. Human breast tumor xenografts that express the tdTomato fluorescent protein in hypoxic regions were orthotopically grown in athymic nude mice and, following tumor removal, were embedded in gelatin with three CV fiducial markers. Two vertical markers allowed an easy coregistration of the optical and ion images in 2D while the additional diagonal marker was used during 3D volume reconstruction of MSI data. Fresh tumor sections of 2 mm thickness were imaged by bright field and fluorescence microscopy in order to visualize tumor boundary and expression of tdTomato red fluorescent protein present in the hypoxic regions of this tumor model (Figure 2a,b). The bright field and fluorescence images were coregistered based on the position of the fiducial markers visible in both images (Figure 2c). The red color of tdTomato was changed into black for better visualization of hypoxic regions. Positive ion MALDI-TOF images were acquired from subsequently cryo-sectioned 10 μm thick tissue sections, detecting the fiducial markers at m/z 262.0 (Figure 2d) and multiple biomolecular ions. An optical image and the ion images were coregistered in Biomap software based on the position of the fiducial markers (Figure 2e). Overlays between MSI images, such as the image of m/z 1198.7 identified as a tryptic peptide ion of actin (Figure 2f), and tissue optical images can subsequently be accurately generated (Figure 2g).

A schematic diagram representing the location of the fiducial markers inside the gelatin block, which allowed proper 3D alignment of multiple ion images acquired by MSI from different sections obtained from the same tumor is shown in Figure 3a. We took advantage of the abundant presence of actin in all tumor cells for the reconstruction of the total tumor volume. Figure 3b shows the 3D reconstructed ion image of the actin tryptic peptide (m/z 1198.7, shown in gray) used for the reconstruction of tumor boundaries. The position of fiducial markers was reconstructed based on the signal of CV detected at m/z 262.0.

The 3D reconstruction of tumor tissue volumes based on the position of the fiducial markers was performed for optical bright field and tdTomato fluorescence microscopic images. Figure 4a shows the 3D reconstruction of tumor tissue volumes obtained from three 2 mm tumor sections. The tumor boundary was reconstructed based on the shape of the tumor tissue visualized in the bright field as shown in Figure 2a. The markers were visualized based on their position in the optical bright field

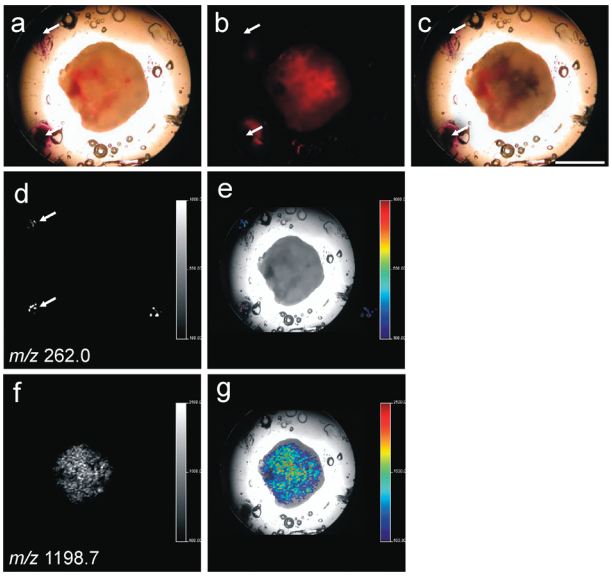

Figure 2. Multimodal imaging of MDA-MB-231-HRE-tdTomato-expressing breast tumor xenograft tissue sections. Optical microscopic imaging combined with MSI. (a) Optical image of a representative 2 mm thick tumor section. White arrows indicate the fiducial markers. (b) Fluorescence image of the distribution of tdTomato inside hypoxic tumor regions. (c) Coregistration of optical and fluorescence images based on the position of the fiducial markers. The red color of tdTomato was changed to black for better visualization of the hypoxic region inside tumor tissue. (d) Ion image of the cresyl violet fiducial marker at m/z 262.0. (e) Coregistration of optical image and MSI image of the cresyl violet marker. (f) MSI image of the actin tryptic-peptide at m/z 1198.7. (g) Coregistration of optical image and MSI image of the actin tryptic-peptide ion at m/z 1198.7. Scale bar, 500 μm.

images (Figure 2a). The tdTomato red fluorescent protein signal (shown in Figure 2b) was used to reconstruct the position and volume of the hypoxic regions present inside the tumor. Figure 4b shows the 3D reconstruction performed based on the H&E stained tissue sections of the same tumor. Figure 4c presents the 3D reconstruction of the MSI data obtained from the same tumor. The distribution of the hemoglobin tryptic peptide (m/z 1529.7, shown in green) was generated to show the localization of hemoglobin inside the tumor, while the distribution of the tdTomato tryptic peptide (m/z 2225.0, shown in red) revealed the position of hypoxic regions inside the tumor. The ion image of the actin tryptic peptide (m/z 1198.7, shown in gray) was used to reconstruct the tumor boundary. Fiducial markers (m/z 262.0, shown in yellow) were used for alignment of 10 MSI 2D data sets.

The ion intensity normalization for 3D reconstruction of the MSI data was performed by using the MSI-detected intensity of the CV marker in each one of the 2D tissue sections. The concentration of each CV marker was constant across the entire gelatin block. The CV ion of each individual sectional 2D MSI image at m/z 262.0 was visualized in BioMap software, and the generated MSI image at m/z 262.0 was exported as a portable network graphics (PNG) file. Each straight marker in each sectional MSI image at m/z 262.0 was detected by using an active shape model ("snake" or ASM model) in the Gradient Vector Flow Active Contour Toolbox written in Matlab.[24] An average intensity of all markers within each section and across all sections was calculated using Matlab. The differences between individual and averaged CV intensities across all sections and within each section were corrected in the reconstructed 3D data set, and the intensities of ions of interest such as actin, tdTomato, or hemoglobin were adjusted accordingly. Normalized 2D images of different ions were intersectionally aligned according to the positions of the corresponding CV markers. Then aligned 2D sectional MSI images were interpolated and rendered into a 3D volume, which was displayed using the Amira software.

The coregistration of the 3D volumes obtained from bright field/fluorescence microscopy data (Figure 4a) and MSI data (Figure 4c) is shown in Figure 5a and from the H&E histological staining (Figure 4b) and MSI data (Figure 4c) in Figure 5b. A vertical fiducial marker based rigid registration and a tumor shape based warping was applied to bright field/fluorescence microscopy data in order to perform 3D coregistration of these different modalities.

This example demonstrates the added value of an MS compatible fiducial marker based coregistration in a multimodal molecular imaging experiment. It allows for the accurate reconstruction and registration of 3D tissue volumes without damage to the tissue itself based on the physicochemical properties of the fiducial markers detected in all imaging modalities employed in this study.

Multimodal molecular imaging, including bright field/fluorescence imaging, MSI, and histological imaging, of the same tissue requires the presence of clear fiducial markers for coregistration, ion intensity normalization, and 3D reconstruction of these different modalities. PS provided an intense red color, no diffusion after ethanol treatment, and exhibited good ionization properties in negative ion mode but due to its chemical structure did not produce any signal in positive ion mode. CV had an intense violet color, had good fluorescence

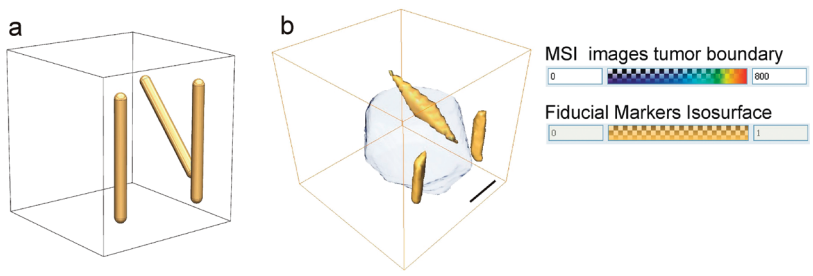

Figure 3. Application of fiducial markers for 3D reconstruction of MSI data. (a) Schematic representation of the position of three markers inside the gelatin block. (b) 3D reconstruction of ion images of the actin tryptic-peptide at m/z 1198.7, which was used for 3D reconstruction of the tumor boundary. The cresyl violet ion images were used for alignment of multiple 2D sections of the tumor imaged by MSI. Scale bar, 500 μm.

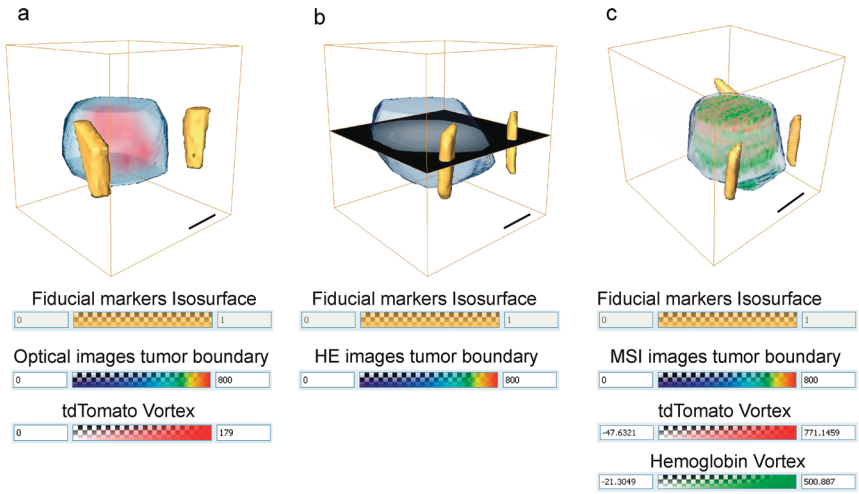

Figure 4. Application of fiducial markers for 3D reconstruction of optical imaging and MSI data. (a) 3D reconstruction of the hypoxic region based on optical microscopy images from 2 mm thick tumor sections. The fluorescence signal from tdTomato is shown in red. The tumor boundary was reconstructed based on the tissue shape visualized by optical microscopy. (b) 3D reconstruction of H&E stained tumor sections. The tumor boundary was reconstructed based on the tissue shape obtained from H&E stained images. (c) 3D reconstruction of the tumor imaged by MSI. The actin tryptic-peptide at m/z 1198.7 was used for reconstruction of the tumor boundary. The hemoglobin tryptic-peptide at m/z 1529.7 shown in green was used to visualize the distribution of blood inside the tumor. The tdTomato tryptic-peptide at m/z 2225.0 (in red) was used for reconstruction of the hypoxic region inside the tumor. Scale bars, 500 μm.

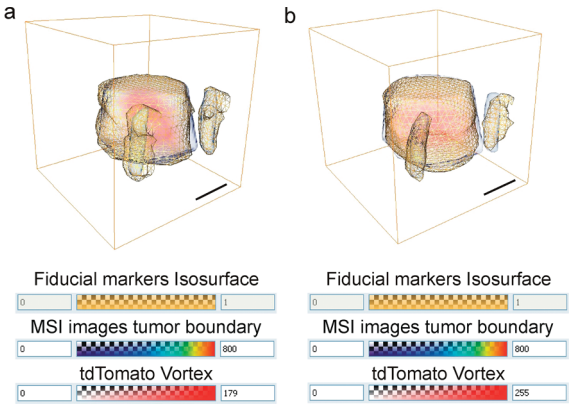

Figure 5. Coregistration of 3D images from optical imaging, H&E imaging, and MSI based on the position of the fiducial markers. (a) Coregistration of MSI data (gray) and optical imaging data (tumor boundary shown as mesh, hypoxic region in red). (b) Coregistration of MSI data (actin in gray, tdTomato in red) and H&E imaging data (mesh). Scale bars, 500 μm.

properties, and ionized well in positive ion mode but dissolved slightly in ethanol during tissue washing and did not ionize in negative ion mode. The 1:1 mixture of CV and PS fulfilled all requirements for a multimodal marker for imaging in both positive and negative ion modes, showed adequate stability during washing, and had excellent optical properties. The fluorescence properties of CV can be used for coregistering fluorescence images, such as for example images of tdTomato fluorescent protein, which is expressed under hypoxic conditions in the studied tumor model.

BB ionized in both positive and negative ion modes and could be used as a fiducial marker. However, its pH dependent color change to yellow color reduced its practicability due to poor contrast in the optical images taken after matrix deposition. In this case, ion images can be coregistered with optical images of the tissue obtained before matrix deposition.

In the future, coregistration of different imaging modalities may allow an image-based evaluation of disease boundaries based on molecular properties determined by MRI, histology, IHC, or MSI and can be applied in preclinical studies to measure the effectiveness of new molecular therapies. Moreover, a range of biomedical imaging applications may benefit from multimodal molecular histology, including measuring the effects of laser,[25] radiofrequency,[26] or ultrasound[27] thermal ablation therapies. Their successful application and interpretation will be crucially dependent on accurate coregistration. The fiducial markers and their application described in this manuscript will be key in the automated generation of high-throughput molecular volumes.

CONCLUSIONS

Fiducial markers such as cresyl violet, Ponceau S, and bromophenol blue proved useful for multimodal image coregistration, 3D image alignment, MSI ion intensity normalization, and 3D reconstruction. Our data demonstrate that a 1:1 mixture of cresyl violet and Ponceau S is optimal for combining bright field, fluorescence, and histological imaging with positive and negative ion MSI, resulting in coregistered, 3D-reconstructed, fused multimodal image data sets.

ASSOCIATED CONTENT

Supporting Information

Additional information as noted in text. This material is available free of charge via the Internet at http://pubs.acs.org.

AUTHOR INFORMATION

Corresponding Author

*Kristine Glunde: address, The Russell H. Morgan Department of Radiology and Radiological Science, The Johns Hopkins University School of Medicine, 212 Traylor Building, 720 Rutland Avenue, Baltimore, MD 21205; phone, +1-410-614-2705; fax, +1-410-614-1948; e-mail, kglunde@mri.jhu.edu. Ron M. A. Heeren: address, FOM Institute AMOLF, Science Park

104, 1098 XG Amsterdam, The Netherlands; phone, +31-20-486 7547100; fax, +31-20-7547290; e-mail, heeren@amolf.nl.

Notes

The authors declare no competing financial interest.

■ ACKNOWLEDGMENTS

R. M. A. Heeren and K. Glunde share last authorship of this manuscript. We thank Drs. Paul T. Winnard, Jr., Venu Raman, and Zaver M. Bhujwalla for providing the MDA-MB-231-HRE-tdTomato breast cancer cell line. This work is part of the research program of the "Stichting voor Fundamenteel Onderzoek der Materie (FOM)", which is financially supported by the "Nederlandse Organisatie voor Wetenschappelijk Onderzoek (NWO)". We gratefully acknowledge financial support from NIH Grant R01 CA134695. The authors also gratefully acknowledge continued support from The Netherlands Proteomics Centre (NPC). We thank Henk-Jan Boluijt for assistance with graphical designs.

■ REFERENCES

(1) Amstalden van Hove, E. R.; Blackwell, T. R.; Klinkert, I.; Eijkel, G. B.; Heeren, R. M.; Glunde, K. *Cancer Res.* **2010**, *70*, 9012−9021.
(2) Sinha, T. K.; Khatib-Shahidi, S.; Yankeelov, T. E.; Mapara, K.; Ehtesham, M.; Cornett, D. S.; Dawant, B. M.; Caprioli, R. M.; Gore, J. C. *Nat. Methods* **2008**, *5*, 57−59.
(3) Altelaar, A. F.; Luxembourg, S. L.; McDonnell, L. A.; Piersma, S. R.; Heeren, R. M. A. *Nat. Protoc* **2007**, *2*, 1185−1196.
(4) Djidja, M. C.; Claude, E.; Snel, M. F.; Scriven, P.; Francese, S.; Carolan, V.; Clench, M. R. *J. Proteome Res.* **2009**, *8*, 4876−4884.
(5) Khatib-Shahidi, S.; Andersson, M.; Herman, J. L.; Gillespie, T. A.; Caprioli, R. M. *Anal. Chem.* **2006**, *78*, 6448−6456.
(6) Chughtai, K.; Heeren, R. M. A. *Chem. Rev.* **2010**, *110*, 3237−3277.
(7) Shaner, N. C. *Nat. Biotechnol.* **2004**, *22*, 1567−1572.
(8) Winnard, P. T. Jr.; Kluth, J. B.; Raman, V. *Neoplasia* **2006**, *8*, 796−806.
(9) Kakkad, S. M.; Solaiyappan, M.; O'Rourke, B.; Stasinopoulos, I.; Ackerstaff, E.; Raman, V.; Bhujwalla, Z. M.; Glunde, K. *Neoplasia* **2010**, *12*, 608−617.
(10) Eberlin, L. S.; Ifa, D. R.; Wu, C.; Cooks, R. G. *Angew. Chem., Int. Ed.* **2010**, *49*, 873−876.
(11) Chen, R.; Hui, L.; Sturm, R. M.; Li, L. *J. Am. Soc. Mass Spectrom.* **2009**, *20*, 1068−1077.
(12) Andersson, M.; Groseclose, M. R.; Deutch, A. Y.; Caprioli, R. M. *Nat. Methods* **2008**, *5*, 101−108.
(13) Sidman, R. L.; Kosaras, B.; Misra, B.; Senft, S. 2004.
(14) Crecelius, A. C.; Cornett, D. S.; Caprioli, R. M.; Williams, B.; Dawant, B. M.; Bodenheimer, B. *J. Am. Soc. Mass Spectrom.* **2005**, *16*, 1093−1099.
(15) Lazebnik, R. S.; Lancaster, T. L.; Breen, M. S.; Lewin, J. S.; Wilson, D. L. *IEEE Trans. Med. Imaging* **2003**, *22*, 653−660.
(16) Breen, M. S.; Lazebnik, R. S.; Wilson, D. L. *Ann. Biomed. Eng.* **2005**, *33*, 1100−1112.
(17) Humm, J. L.; Ballon, D.; Hu, Y. C.; Ruan, S.; Chui, C.; Tulipano, P. K.; Erdi, A.; Koutcher, J.; Zakian, K.; Urano, M.; Zanzonico, P.; Mattis, C.; Dyke, J.; Chen, Y.; Harrington, P.; O'Donoghue, J. A.; Ling, C. C. *Med. Phys.* **2003**, *30*, 2303−2314.
(18) Breen, M. S.; Lancaster, T. L.; Wilson, D. L. *Comput. Med. Imaging Graphics* **2005**, *29*, 405−417.
(19) McGrath, D. M.; Vlad, R. M.; Foltz, W. D.; Brock, K. K. *Med. Phys.* **2010**, *37*, 2321−2328.
(20) Rouviere, O.; Reynolds, C.; Le, Y.; Lai, J.; Roberts, L. R.; Felmlee, J. P.; Ehman, R. L. *J. Magn. Reson. Imaging* **2006**, *23*, 50−59.
(21) Raman, V.; Artemov, D.; Pathak, A. P.; Winnard, P. T. Jr.; McNutt, S.; Yudina, A.; Bogdanov, A. Jr.; Bhujwalla, Z. M. *Cancer Res.* **2006**, *66*, 9929−9936.
(22) Glunde, K.; Shah, T.; Winnard, P. T. Jr.; Raman, V.; Takagi, T.; Vesuna, F.; Artemov, D.; Bhujwalla, Z. M. *Cancer Res.* **2008**, *68*, 172−180.
(23) Jiang, L.; Greenwood, T. R.; Amstalden van Hove, E. R.; Chughtai, K.; Raman, V.; Winnard Jr., P.; Heeren, R. M. A.; Artemov, D.; Glunde, K. *NMR Biomed.* In press.
(24) Xu, C.; Prince, J. L. *IEEE Trans. Image Process.* **1998**, *7*, 359−369.
(25) Morrison, P. R.; Jolesz, F. A.; Charous, D.; Mulkern, R. V.; Hushek, S. G.; Margolis, R.; Fried, M. P. *J. Magn. Reson. Imaging* **1998**, *8*, 57−63.
(26) Breen, M. S.; Lancaster, T. L.; Lazebnik, R. S.; Nour, S. G.; Lewin, J. S.; Wilson, D. L. *J. Magn. Reson. Imaging* **2003**, *18*, 90−102.
(27) Hazle, J. D.; Diederich, C. J.; Kangasniemi, M.; Price, R. E.; Olsson, L. E.; Stafford, R. J. *J. Magn. Reson. Imaging* **2002**, *15*, 409−417.